Materials Advances

ROYAL SOCIETY OF CHEMISTRY

PERSPECTIVE

View Article Online
View Journal | View Issue

Cite this: *Mater. Adv.*, 2023, 4, 5420

An oxygen-generating metal organic framework nanoplatform as a "synergy motor" for extricating dilemma over photodynamic therapy

Meihong Zhang,†[a] Yixian Zhou,†[b] Biyuan Wu,†[b] Chao Lu,*[a] Guilan Quan,*[a] Zhengwei Huang,*[a] Chuanbin Wu[a] and Xin Pan[b]

Received 9th July 2023,
Accepted 8th October 2023

DOI: 10.1039/d3ma00382e

rsc.li/materials-advances

Photodynamic therapy, a non-invasive tumor treatment method, selectively kills tumor cells through reactive oxygen species (ROS) generated by photosensitizers. However, traditional photodynamic therapy merely utilizes the limited oxygen in the tumor microenvironment as the source of ROS, resulting in insufficient ROS for activating the eradication of tumors. Meanwhile, given that most photosensitizers bear potently hydrophobic planar conjugate structures which are prone to aggregate spontaneously in water, the efficiency of producing ROS will be reduced upon aggregation caused quenching (ACQ). Thereby, the development of photodynamic therapy is limited by the above two bottlenecks. Metal organic frameworks (MOFs) were reported to possess ample potential for photodynamic therapy in cancer treatment, where diverse metal ions converted the overexpressed endogenous hydrogen peroxide in tumor tissues into ROS *via* Fenton reactions/Fenton-like reactions, which effectively surmounted the hypoxic environment of tumors and avoided the immunosuppression and treatment resistance in such a state. Moreover, the unique pores of MOFs could inhibit the ACQ effect of photosensitizers in the physiological environment *via* steric effects, ultimately improving the efficacy of photodynamic therapy. Furthermore, MOFs could co-load photosensitizers and chemotherapeutic drugs, which will release both counterparts to synergistically kill tumor cells after the degradation of MOFs in the tumor microenvironment. In general, MOFs are a promising "synergy motor" nanoplatform for overcoming the bottleneck issues of photodynamic therapy. We believe that this work will provide a new insight into tumor photodynamic therapy.

1. Introduction

Malignant tumors seriously endanger human health, and the number of cancer deaths has been continuously increasing in recent years all over the world. According to global cancer statistics 2020, there are an estimated 19.3 million people with new cancer cases and nearly 10.0 million cancer deaths all around the world. Female breast cancer has surpassed lung cancer as the most commonly diagnosed cancer, with an estimated 2.3 million new cases, followed by lung cancer (2.2 million), colorectal cancer (1.9 million), prostate cancer (1.4 million), and stomach cancer (1.1 million), and lung cancer remains the leading cause of cancer deaths, with an estimated 1.8 million deaths, followed by colorectal cancer (0.9 million), liver cancer (0.8 million), stomach cancer (0.8 million), and female breast cancer (0.7 million).[1]

At present, surgery, radiotherapy, and chemotherapy, as well as a combination of the above therapies are the main treatments for tumors. However, there are some limitations in these therapies, for instance, surgery is often associated with large trauma, difficulties in removing the small metastatic lesion and the potential for recurrence.[2] Severe side effects are caused by the inability of the drug to be target-delivered to the tumor when treating cancer with chemotherapy.[3] Radiotherapy can not only damage normal tissues and organs of patients but easily induce drug resistance.[4] Combined therapies also face similar problems. Therefore, there is an urgent need to develop a new treatment method that breaks through the above limitations.

2. Photodynamic therapy is promising in cancer treatment

Photodynamic therapy (PDT) is a promising approach to overcome the limitations of surgery, radiotherapy and chemotherapy, which can minimize accidental damage to normal cells. This is because photosensitizers can be selectively enriched at tumor

[a] *College of Pharmacy, Jinan University, Guangzhou 510632, P. R. China. Tel: +86-020-39943117*
[b] *College of Pharmacy, Sun Yat-sen University, Guangzhou 510275, P. R. China*
† These authors contributed equally.

sites, and because the scope of killed cells will be controlled through guiding the location and duration of laser irradiation.[5,6] In addition, employing generating ROS, it drives cancer cells towards apoptosis and necrosis *via* stimulating the photosensitizer using light with a specific wavelength,[7–9] which is a major area of interest within the field of cancer treatment. Herein, ROS is defined as a generic term for a large family of reactive species derived from molecular oxygen (O_2),[10] which can be classified into superoxide anion ($O_2^{\bullet -}$), hydrogen peroxide (H_2O_2), and hydroxyl radical ($HO^{\bullet}$); besides, diverse peroxides like those of lipids, proteins and nucleic acids are also included,[11] but these are less relevant to the species utilized in PDT.

Generally, photosensitizers are in the ground singlet state, where all electrons rotate in pairs in low-energy orbitals, and when irradiated with a laser of the appropriate wavelength, the activated singlet state of photosensitizers reverses the rotation of the activated electrons to generate the triplet state, and hence two molecular mechanisms are involved in the triplet state of the photosensitizers.[12] Type I mechanisms: The main species include superoxide anion ($O_2^{\bullet -}$), hydroxyl radical ($OH^{\bullet}$), hydrogen peroxide (H_2O_2), *etc.* They are commonly generated *via* a one-electron oxidation–reduction reaction with a neighboring oxygen molecule, through electron transfer from an excited triplet state; Type II mechanism: Singlet oxygen ($^1O_2$) can be harvested from the excited triplet state *via* energy transfer, which is involved in the most commonly used organic photosensitizers[13] (Fig. 1). Of note, both mechanisms demand O_2 as the substrate for the reaction. Currently, most photosensitizers induce PDT through the generation of $^1O_2$ by the type II mechanism, and thus, $^1O_2$ is regarded as the primary kind of ROS produced by photosensitizers.

There are three major mechanisms of PDT for killing tumor cells.[15] First, proteins and phospholipids oxidized by ROS can lead to reversible phototoxicity toward the subcellular structures (mitochondria, lysosomes, Golgi apparatus, *etc.*). Second, ROS can stimulate the immune system and trigger specific immunity through inducing local inflammation to achieve long-term tumor control. Third, photosensitizers can also impair epithelial cells of the microvasculature, and increase vascular permeability and occlusion, resulting in tumor growth inhibition. Compared with traditional cancer treatment approaches, PDT has excellent tissue selectivity and can optionally induce tumor cell necrosis without harming normal tissues, which greatly reduces side effects while improving treatment effects.

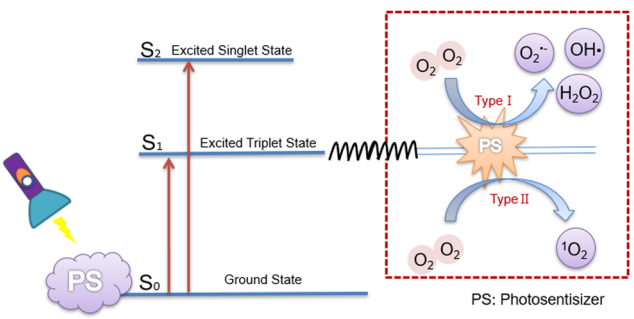

Fig. 1 Two types of mechanism of ROS generation by photosensitizers.[14]

In the past few decades, the applications of PDT have been boosted by virtue of the development of photosensitizers. It is well known that the ideal clinical photosensitizers should meet the following requirements: (i) can be dissolved and not aggregate in the aqueous environment and have minimal dark toxicity and only be toxic in the presence of a laser with the appropriate wavelength;[16] (ii) should be promptly metabolized and excreted from the body upon completion of the treatment cycle;[17] (iii) have a high absorption coefficient in the spectral range of 600–800 nm with maximum photo-transparency through tissue and the absorption band of the photosensitizers should not be allowed to overlap with the absorption band of the endogenous dyes to minimize experimental errors.[18]

With the purpose of satisfying the above prerequisites, numerous photosensitizer candidates have been designed and synthesized. Nevertheless, not all of them can fortunately witness a clinical translation. Currently, there are multiple types of photosensitizers applied in clinics, such as porfimer sodium, 5-aminolevulinic acid, benzoporphyrin monocyclic derivative acid A, and zinc phthalocyanine, *etc.* (Table 1). PDT has shown a satisfactory effect on the treatment of bladder cancer, non-small cell lung cancer, head and neck cancer, skin cancer and glioblastoma,[19] which can prolong the survival period and significantly improve the life quality of patients. In addition, the combination of PDT with other treatment methods,[20,21] especially with chemotherapy, has provided considerable potential for application.

3. Developmental bottleneck of PDT

Despite the great advantages and potential, the clinical application of PDT is still confined by the following obstacles. (i) The majority of conventional photosensitizers are triggered by short activation wavelengths. This consequently leads to poor tissue penetration, which renders the clinical application of PDT constrained to superficial tumors.[29] (ii) PDT exacerbates hypoxia in the tumor microenvironment, owing to oxygen depletion and vascular closure effects, which ultimately trigger tumor metastasis and tumor recurrence.[30] (iii) There are tumor recognition challenges.[31] (iv) Hydrophobic photosensitizers accumulate non-specifically in the skin upon photodynamic therapy, causing cutaneous photosensitization.[32] (v) Insufficient O_2 levels. (vi) Instable photosensitizer delivery. Obstacles (i–iv) have been well or partly overcome, however (v) and (vi) have not been well addressed. According to the principle of PDT, to ensure its therapeutic efficacy, sufficient O_2 levels and stable photosensitizer delivery are of great significance. Nevertheless, hypoxia in tumor microenvironments and photosensitizers with ACQ effects limit the development of PDT, and are bottlenecks.

3.1 Solutions of obstacles (i)–(iv)

Fortunately, some of the above-mentioned obstacles are now being effectively addressed (Fig. 2). (i) X-rays permit non-

Table 1 Summary of typical photosensitizers[22–28] (part of the content from PharmSnap)

Generations	Categories	Photosensitizers	Indications	Present situation
First	Hematoporphyrin	Porphyrin sodium	Lung cancer, esophageal cancer, bladder cancer, brain cancer, ovarian cancer	Marketed (1995)
	Photoporphyrin precursors	5-Aminolevulinic acid	Actinic keratosis, basal cell carcinoma, head-neck cancer and diagnosis	Marketed (1999)
		5-Aminolevulinic acid hexylester	Bladder cancer diagnosis	Marketed (2010)
Second	Benzo porphyrin	Benzo porphyrin monocyclic derivative acid A	Pathological myopia, histoplasmosis, bacteriopathy, hygroscopic aging-relation, macular degeneration	Marketed (2000)
	Phthalocyanine	Zinc phthalocyanine	Skin cancer, breast cancer, T-cell non-Hodgkin's lymph disease	Termination (clinical trial I)
	Dihydroporphine /entry>	Talaporfin	Brain cancer, lung cancer	Marketed (2003)
	Erythrosine	Purlytin	Breast cancer, arteriovenous Fistula	Clinical trial III

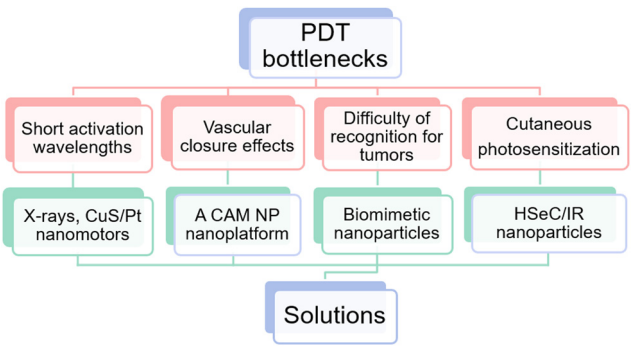

Fig. 2 A summary of bottlenecks and solutions for PDT.

invasive treatment of deep tumors since they experience relatively little absorption or scattering *in vivo*.[33] Similarly, CuS/Pt Janus nanoparticles can also penetrate the deep tumor.[34] (ii) Luan *et al.*[35] reported a CAM NP nanoplatform, which integrated chlorine e6 (Ce6), axitinib (AXT), and dextro-L-methyl tryptophan (1MT). Among these, AXT could inhibit VEGF to reduce abnormal tumor blood vessels and increase blood perfusion, hence making vascular normalization. (iii) Biomimetic nanopreparations are becoming a hot research topic since they can substantially enhance the targeting of tumors. For instance, Duo *et al.*[36] developed platelet-mimicking MnO_2 nanozyme/AIEgen composites (PMD) for PDT management, and the resultant biomimetic nanoparticles (NPs) exhibited excellent tumor-targeting properties. (iv) Li *et al.*[37] designed HSeC/IR nanoparticles, which consist of hyaluronic acid (HA), photosensitizer chlorin e6 (Ce6), and NIR photothermal dye IR780. The results have shown that the skin damage during PDT treatment could be severely suppressed. Still, there are no satisfactory and robust solutions for hypoxia in tumor sites and photosensitizer instability.

3.2 Obstacle (v): insufficient O_2 levels

Hypoxia in the tumor microenvironment suppresses the production of ROS and induces chemoresistance. It is important that sufficient O_2 should serve as the substrate for PDT, whereas, O_2 deficiency is a typical feature in the majority of solid tumors. Due to the rapid growth of the tumor and the abnormal microvascular system in the tumor interstitium, severe imbalance between O_2 consumption and supply at the tumor site is yielded.[38] Studies have shown that when the partial pressure of O_2 in tumor tissue was lower than 15–35 mmHg, the number of various cancer cells killed by PDT would be significantly reduced.[39] Noticeably, the activation of PDT will further consume O_2 and aggravate the O_2 deficiency in the tumor. The lack of O_2 in the tumor microenvironment results in the inability of conventional PDT to provide sufficient ROS continuously.

Worse still, hypoxia-inducible factor-1α (HIF-1α), can manipulate various essential biological processes required for adapting to such a hypoxic environment, including glucose metabolism, cell proliferation and angiogenesis, *etc.* (Fig. 3).[40] For instance, it participates in glucose metabolism through the overexpression of glucose transporters (GLUTs) in the glycolysis pathway to satisfy the energy requirements of tumor growth.[41] Simultaneously triggering several angiogenic factors, such as vascular endothelial growth factor (VEGF), HIF-1α consequently stimulates the formation of new blood vessels that can provide abundant oxygen for tumor growth.[42]

The expression of apoptosis suppressor genes, such as an X-linked inhibitor of apoptosis protein (XIAP), and multidrug resistance genes like miniRNA-27a (miR-27a)[43] will be also activated by excessive accumulation of HIF-1α in the hypoxic environment, which results in a strong degree of chemotherapy resistance.[44] It has been shown in recent research that improving the hypoxic state of the tumor microenvironment or inhibiting HIF-1α could strengthen the sensitivity of tumor cells to chemotherapy, and thus reverse the effects of therapeutic resistance[45–47] (Fig. 3). Subsequently, PDT exhibits restricted possibilities in combination with chemotherapy, on account of HIF-1α-induced resistance.[48]

In summary, providing sufficient O_2 is an indispensable prerequisite for the maximization of PDT efficacy.

3.3 Obstacle (vi): ACQ of photosensitizers

It should be noticed that the ACQ effect predominantly applies to hydrophobic organic photosensitizers rather than inorganic ones. The performance of hydrophobic photosensitizers is constrained by their ACQ properties. At present, 90% of the photosensitizers used clinically (and more than 90% of those

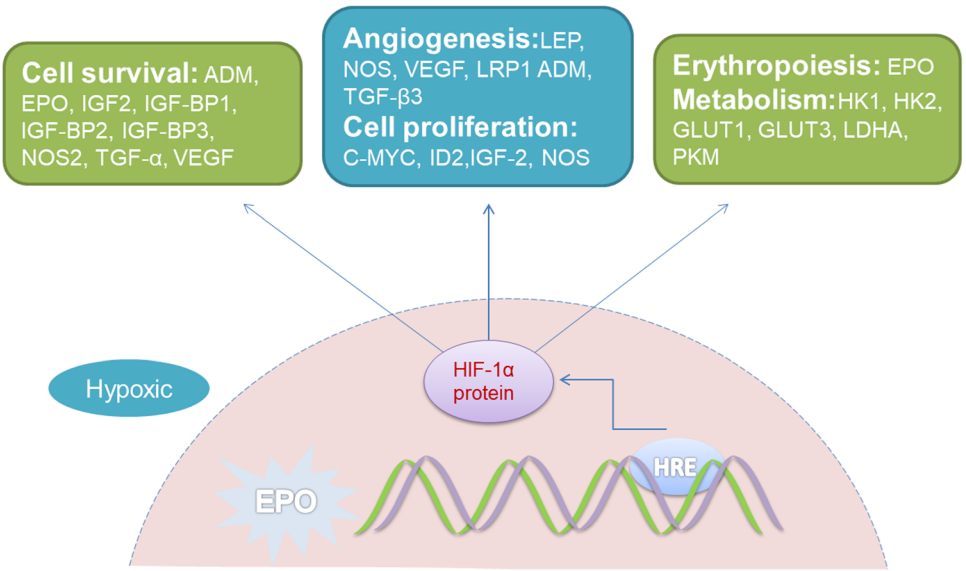

Fig. 3 Representative HIF-1α regulatory genes and their effects on cancer progression under hypoxic conditions. EPO, erythropoietin gene; HRE, hypoxia response elements; LEP, leptin; NOS, nitric oxide synthase; VEGF, vascular endothelial growth factor; LRP1, LDL-receptor-related protein 1; ADM, adrenomedullin; TGF-β3, transforming growth factor-β3; EPO, erythropoietin; HK1, hexokinase 1; HK2, hexokinase 2; GLUT1, glucose transporter 1; GLUT3, glucose transporter 3; LDHA, lactate dehydrogenase; PKM, pyruvate kinase M; IGF2, insulin-like growth factor 2; IGF-BP2, IGF-factor-binding protein 2; IGF-BP3, IGF-factor-binding protein 3; TGF-α, transforming growth factor α; C-MYC, myelocytomatosis virus oncogene cellular homolog; ID2, DNA-binding protein inhibitor.[40]

under development) are hydrophobic molecules with a planar conjugated structure. Due to the powerful π–π interaction between these molecules, a drastically vigorous aggregation tendency occurs upon contact with the aqueous physiological environment.[49] This will give rise to the following inferiorities.

Firstly, the aggregation of photosensitizers *in vivo* prevents them from adequately being in contact with O_2 molecules, which seriously influences the yield of ROS. Secondly, the large size of the aggregates is detrimental to transmembrane transport, which reduces the concentration of the photosensitizer in the tumor tissue. Thirdly, prone to forming H-aggregates (face to face parallel stacking between molecules), the aggregation of photosensitizers ultimately leads to non-radiative dissipation of energy, which results in decreased or even complete inability to produce ROS[50] (Fig. 4).

Hence, it is necessary to explore an ideal delivery system that ensures photosensitizers exist in the form of non-aggregates in the physiological environment and expedites exposure to O_2 molecules in order to achieve excellent PDT effects.

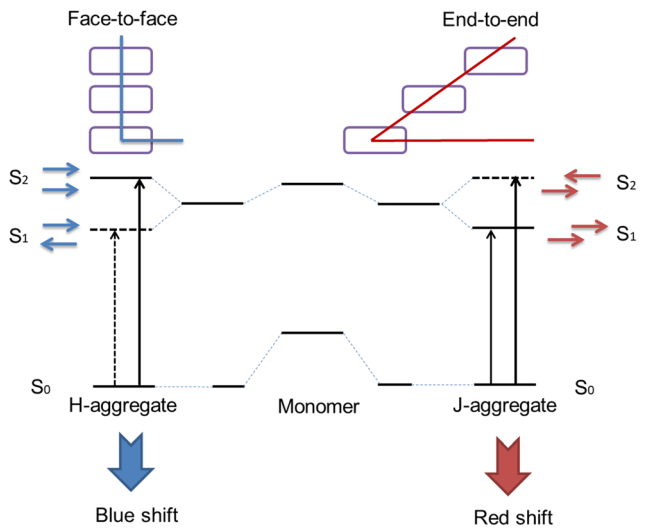

Fig. 4 Schematic presentation of the mechanisms of H-aggregate and J-aggregate formation.[51]

4. Current efforts to address the bottlenecks

We need to open the perspective to address two major issues to promote the application of PDT in oncology treatment, *viz.* the hypoxic microenvironment and ACQ effects of the photosensitizer. To address these problems, perfluorinated carbons, hemoglobin, *etc.* as a co-delivery platform of O_2 and photosensitizers were designed. Cheng *et al.*[52] prolonged the performance duration of $^1O_2$ *via* a nanoemulsion co-delivery system prepared by perfluorinated carbons that physically load O_2 and photosensitizer IR-780. Luo *et al.*[53] increased the O_2 partial pressure of tumor tissue and improved the effect of PDT through biomimetic red blood cells co-loading hemoglobin (equilibrated with O_2) and indocyanine green (ICG). Sheng *et al.*[54] prepared perfluorooctyl bromide (PFOB) integrated with ICG in a nanoliposome structure. Due to the excellent O_2 carrying ability of PFOB, tumor hypoxia was effectively improved.

Regarding the above systems, O_2 was directly loaded, and the photosensitizer was accommodated in a restricted space

that could reduce the trend to aggregate. Therefore, these techniques to some degree fulfilled the two requirements. However, there is a considerable dilemma regarding co-delivery of the O_2 and photosensitizer. On one hand, the O_2-carrying capacity of the proposed carriers was limited, which could not long-term alter the hypoxic status. On the other hand, the steric refraining attributes of the carriers were insufficient to substantially reduce the ACQ phenomenon, where photosensitizers still had a certain probability of colliding and aggregating. In this context, a novel robust strategy to achieve enhanced O_2 levels and reduced photosensitizer's ACQ effects must be developed.

5. To overcome the bottleneck by walking on two legs

With the purpose of developing a credible strategy, a two-tailed logic can be applied for conceptualization. For one thing, the O_2 levels should be elevated, and transforming H_2O_2 *in situ* into O_2 can be considered. For another thing, the ACQ phenomenon should be avoided, which can be achieved by incorporating photosensitizers into porous materials.

5.1 *In situ* transforming H_2O_2 into O_2

H_2O_2 is a metabolic intermediate commonly required by aerobic cells and can be removed directly by the enzyme catalase (CAT), or consumed by reduced glutathione (GSH) to form oxidized glutathione (GSSG) in biological systems, which are favorable to cater for the growth-demand of normal cells.[55] Whereas, most tumor cells show metabolic alterations resulting in the substantial accumulation of H_2O_2 in the tumor microenvironment. This may be associated with the pathways of phosphatidylinositol 3-kinase (PI3K), mammalian target of rapamycin (mTOR), mitogen-activated kinase (MAPK/ERK) as well as HIF, which has been discussed elsewhere.[56]

As suggested by a previous study,[57] it is a common phenomenon that H_2O_2 accumulates in the tumor microenvironment. For example, compared with the average intracellular steady-state concentration of H_2O_2 to be 10.00 nM or less in red blood cells,[58] the concentration of H_2O_2 produced from the HeLa cells was calculated to be 1.99 mM, which was 10^5-fold higher.[59]

A question arises: 'What will the accumulated H_2O_2 do?' The answer is, H_2O_2 can be utilized as raw materials to produce O_2 through Fenton reactions.

The classical Fenton reactions refer to the reaction between ferrous ions (Fe^{2+}) and H_2O_2 producing O_2 and $OH^{\bullet}$, as discovered by the French scientist Fenton in 1894. In recent years, researchers have found that similar reactions catalyzed by ferric ions (Fe^{3+})[60] or other metal ions like cupric ions (Cu^{2+}),[61] manganese ions (Mn^{2+}),[62] cobalt ions (Co^{2+})[63] and silver ions (Ag^{+})[64] or even organic molecules like benzoyloxycinnamaldehyde (BCA)[65] can also obtain a favorable outcome, which are called Fenton-like reactions. For clarity, the reaction formulae of Fe^{2+}/Fe^{3+} and H_2O_2 are as follows:[66]

$$Fe^{3+} + H_2O_2 \rightarrow Fe^{2+} + O_2 + 2H^{+}$$

$$Fe^{2+} + H_2O_2 \rightarrow Fe^{3+} + (OH)^{-} + OH^{\bullet}$$

$$Fe^{2+} + O_2 \rightarrow Fe^{3+} + O_2^{\bullet}$$

Through Fenton reactions or Fenton-like reactions, the accumulated H_2O_2 in the tumor microenvironment can be converted into O_2 and $OH^{\bullet}$ *in situ*. Importantly, O_2 can alleviate the hypoxia in a tumor microenvironment for PDT. Additionally, $OH^{\bullet}$ can synergize with ROS (mainly $^1O_2$) generated by PDT to peroxidize unsaturated fatty acids, and decompose proteins, nucleic acids, and polysaccharides, which further impairs cell membranes and ultimately kills tumor cells.[67]

The rationale of Fenton/Fenton-like reactions in tumor cells has been widely proved in various studies (Fig. 5). Herein, nanoformulations were involved, and the reason is as follows. The biosafety of metal ions *in vivo* plays a decisive role in their further clinical translation. Generally, metal ions are continually released in conventional formulations, which will accumulate in non-tumor tissues, hence causing further damage to patients. This scenario will be worse for some toxic heavy metal ions, such as Cu^{2+}, Co^{2+}, and Ag^{+}.[68] Therefore, it is of utmost importance to realize metal ion controlled release and efficiency accumulation at the lesion site. To this aim, nanoformulations with controlled release profiles can be considered.

For instance, Tan *et al.*[60] prepared triiron tetraoxide (Fe_3O_4) nanoparticles modified with 5-aminoketovaleric acid–Zn^{2+} on the surface, which provoked Fenton reactions in T24 cancer cells. Hu *et al.*[61] fabricated a supramolecular photosensitive system of O_2–Cu/ZIF-8@ZIF-8@WP6–MB, Cu^{2+} which activated the Fenton-like reactions in HepG2 cells. Feng *et al.*[62] designed stimuli-responsive manganese carbonate–indocyanine green complexes ($MnCO_3$–ICG), and Mn^{2+} ions act as the trigger of Fenton-like reactions in murine 4T1 breast cancer cells. Gong *et al.*[63] synthesized Co-doped Zn-MOF-5 nanoparticles with a high Co doping rate of 60%, and Co^{2+} ions could mediate chemodynamic therapy through Fenton-like reactions in 4T1 cancer cells. Duan *et al.*[64] developed a novel tumor-selective catalytic nanosystem based on

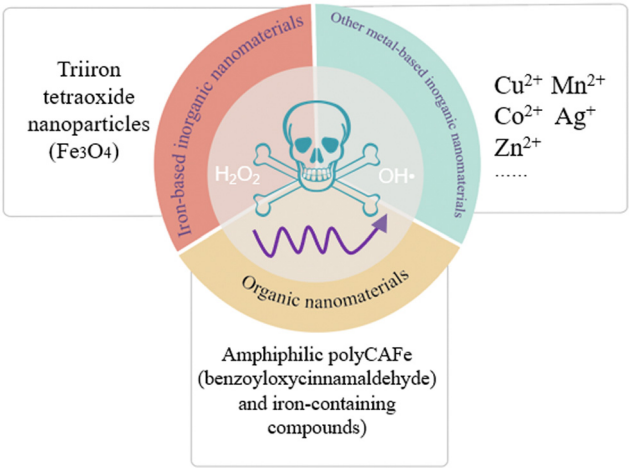

Fig. 5 Diverse nanomaterials induced Fenton reactions or Fenton-like reactions.

an AgNP-mediated Fenton-like reaction, which observed a dose-dependent cytotoxicity in HeLa cells. Ding *et al.*[69] synthesized magnetite nanoparticles loaded with artemisinin and the surface was modified by the long chain of dopamine-ICG-polyethylene glycol, where artemisinin induced Fenton-like reactions in SKOV-3 cells. Kwon *et al.*[65] manufactured amphiphilic PolyCAFe decorated H_2O_2-generating BCA and iron-containing compounds, killing preferentially the colon cancer cell line SW620 and prostate cancer cell line DU145. Also, the above-mentioned studies with satisfactory outcomes have shown that Fenton reactions or Fenton-like reactions can dramatically augment the effect of tumor treatment.

Therefore, the conversion of endogenous H_2O_2 into $OH^{\bullet}$, not only provides continuous ROS for PDT but also assures selectivity, because H_2O_2 is merely abundant in the tumor tissue.

5.2 Incorporating photosensitizers into porous materials

The next task is to solve the ACQ phenomenon of photosensitizers. Previous study has shown that the steric hindrance effect of pores in porous materials could restrict the spatial orientation of the guest molecules, thereby effectively inhibiting molecular aggregation and improving the stability of the guest molecules[70] (Fig. 6). For example, Rengaraj *et al.*[71] synthesized a microporous covalent triazine polymer (CTP) network employed as a potential transport system for anticancer drug delivery like doxorubicin (DOX). Zhang *et al.*[72,73] utilized mesoporous silica Santa Barbara Amorphous-15 (SBA-15) as a delivery carrier, significantly suppressing the aggregation of asarone, and improving the DNA loading capacity *in vivo*.[74] Tu *et al.*[75] designed macroporous pH-sensitive hydrogels, with a rich pore structure, and the payload stability was enhanced.

As for photosensitizers, porous nanomaterials are also demonstrated to have the advantage of overcoming the limitations of aggregation. Feng *et al.*[76] utilized mesoporous zirconia co-delivered DOX and dichloroporphyrin e6. Hao *et al.*[77] utilized amorphous porous manganese phosphate (MnP) nanoparticles loading ICG and an autophagy promoter rapamycin, further decorated with biocompatible poly(glutamic acid). These systems realized improved stability of photosensitizers to different extents.

Thus, encapsulation of photosensitizers into porous materials will be a valuable choice to suppress the ACQ effects, guaranteeing the therapeutic efficiency of PDT.

6. A "synergy motor" metal organic framework is a potential solution

In recent years, the concept of MOFs has become a hotspot. MOFs are porous materials with a periodic network structure formed by the self-assembly of metal ions and organic ligands through ligand bonding.[78] Due to the extensive selection and designability of metal ions and organic ligands, more than 10 000 MOFs have been successfully synthesized so far.[79] Importantly, MOFs have a large specific surface area, high porosity, and present excellent adsorption capacity for small molecule drugs. Besides, since they can collapse and degrade in an acidic environment, the adverse effects of endogenous accumulation in the organism are avoided.[80] Accordingly, MOF-based oncology therapeutic strategies exhibit promising clinical applications.

Compared with other porous material delivery systems, the central metal ions in MOFs exhibit Fenton/Fenton-like reaction catalyzing behavior,[81] which facilitates the continuous conversion of H_2O_2 in the tumor microenvironment into O_2 and $OH^{\bullet}$. Moreover, the metal ions in MOFs are also applied to magnetic resonance imaging (MRI) for imaging-guided precision cancer treatment. Hereby, we will introduce several promising MOFs for anticancer therapy.

6.1 Major categories of MOFs

6.1.1 Fe(II)/Fe(III)-based MOFs. MIL-100(Fe) represents a MOF with a large pore size composed of Fe_3O clusters and benzene-1,3,5-tricarboxylic acid (BTC). Since Fe_3O clusters allow the decomposition of H_2O_2 to generate O_2 through Fenton-like reactions, MIL-100(Fe) is a suitable candidate to simultaneously overcome tumor hypoxia and deliver photosensitizers.[82] Besides, Liang *et al.*[83] developed a nanoparticle composed of ICG and Fe-MOF-5 (I@FM5). The results demonstrated that Fe-MOF-5 possessed the optimal nanoenzyme activity, which was ascribed to the presence of Fe in FM5. It could suppress the proliferation of

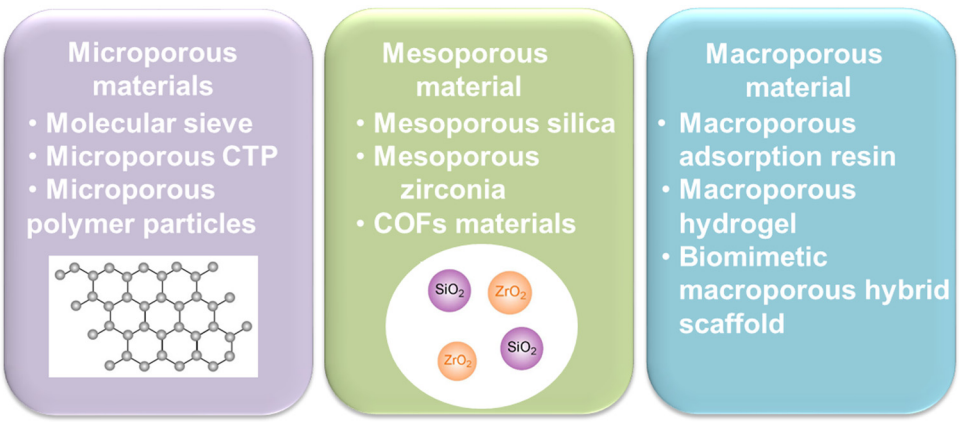

Fig. 6 Classification of porous materials. CTP, covalent triazine polymer; COFs, covalent organic frameworks.

EMT-6 cells through the explosive production of ROS by Fenton-like reactions and exhibit excellent anti-tumor effects.

6.1.2 Cu(II)/Cu(I)-based MOFs. Cu(II)/Cu(I)-MOFs could be applied as a novel tumor-targeting copper supplement with excellent chemical stability, opening the backbone framework, and peculiar near-infrared (NIR) absorption capability for synergistic chemotherapy-photothermal therapy, which made them a suitable candidate for anticancer delivery systems.[84] Therefore, Cai *et al.*[85] reported a biodegradable O_2-loaded CuTz-1@F127 MOF therapeutic platform for enhancing the PDT effect of antitumor agents through overcoming intracellular hypoxia. The Cu(I)-based MOF was capable of activating a Fenton-like reaction to generate $OH^{\bullet}$ and O_2 in the presence of H_2O_2 under NIR irradiation.

6.1.3 Zn-based MOFs. ZIF-8 is a subclass of MOF consisting of zinc ions and 2-methylimidazole (HMIM). Particularly, ZIF-8 has revealed widespread application in the biomedical field and possesses responsiveness in the weakly acidic microenvironment of tumors.[86] Wang *et al.*[87] manufactured a ZIF-8@ssPDA nanosystem for encapsulating Ce6, and disulfide-modified polydopamine (ssPDA) evenly and densely distributed on the ZIF-8 surface. When the structure of the nanosystem disintegrated, the released Ce6 generated ROS, which would present highly efficient cancer-killing through the synergistic effect of PDT and disulfide bond rupture-activated ferroptosis in head and neck cancer management.

6.1.4 Zr-based MOFs. Zr-based porphyrin-MOFs are extremely stable and can be applied directly as a photosensitizer.[88] The high surface area of Zr-MOF, specifically MOF-808, features robustness and water resistance. Its synthetically modifiable pore surface enabled the attachment of photosensitizers in a confined nanospace.[89] Accordingly, Wang *et al.*[90] prepared an integrated theranostics nanoplatform Zr-MOF@PPa/AF@PEG encapsulating photosensitizer pheophorbide-a (PPa). Zr-MOF was considered as a drug carrier with non-phototoxicity and non-dark toxicity. The results demonstrated that it had good biocompatibility and could achieve efficient antitumor effects based on a PDT-chemotherapy cascade process.

6.1.5 Bimetallic MOFs. Bimetallic MOFs possess distinct advantages over monometallic MOFs, owing to their synergistic catalytic effect, structural stability, and abundant active metal catalytic sites, which have raised numerous concerns.[91] $MnFe_2O_4$@MOF-based nanoparticles utilized endogenous H_2O_2 in the tumor microenvironment for sustained O_2 generation by Fenton-like reactions. Meanwhile, the system could decrease the GSH levels, which could reinforce the anti-tumor therapeutic effect of PDT.[92] Similarly, the absorption of Fe/Mn bimetal-doped ZIF-8 was considerably increased through successfully doping with Fe/Mn, which enabled Fe/Mn-ZIF-8 to effectively achieve photocatalytic-driven PDT.[93] Besides, Zhang *et al.*[94] fabricated a novel nanoparticle (NP) comprising Zr-MOF (UiO-66), a biscyclometalated Ir(III) complex, and a dual-responsive polycationic polymer as an anti-tumor delivery nanoplatform (Ir@MOF/P NPs) for effective PDT and cell imaging. It exhibited favorable biocompatibility in the dark and produced abundant ROS upon light irradiation, suggesting that the nanoplatform had the potential to improve the therapeutic performance of PDT to effectively eradicate cancer cells.

Among diverse MOFs, iron-based MOFs with excellent biocompatibility have gained tremendous attention in the field of tumor therapy. This is because they possess the advantages of minimal side effects and high spatial imaging capability that can be used for magnetic resonance imaging (MRI) and photoacoustic imaging (PAI) guided tumor therapy.[95] Most iron-based MOFs are designed to be environmentally (specifically pH) sensitive. Upon contact with acidic sites of tumor regions, the disintegration of the framework takes place, then loaded photosensitizers and Fe^{2+}/Fe^{3+} ions can be released.[96]

6.2 The advantages of MOFs as new drug delivery systems in PDT

6.2.1 Large specific surface area. Given the large specific surface area, high porosity, as well as large pore volume, MOFs exhibit high drug loading.[97] There are three primary strategies for loading MOFs with drugs: encapsulation strategy, direct assembly strategy, and post-synthesis strategy.[98,99] Mn-MOFs were reported that showed satisfactory efficiency for loading drugs. The nitrogen adsorption and desorption experiments have shown that the specific surface areas were 694 $m^2\ g^{-1}$, which could provide massive loading sites for drugs.[100] Coincidentally, MOFs-808 were also reported to have 792 $m^2\ g^{-1}$ specific surface areas, which could effectively load drug.[101]

6.2.2 Alleviating the hypoxic microenvironment. From the above discussion, we realized that MOFs alleviate the hypoxic tumor microenvironment through multiple pathways. Fe(II)/Fe(III)-based MOFs and Cu(II)/Cu(I)-based MOFs were generally regarded as the substrate of H_2O_2, which could generate ROS through Fenton/Fenton-like reactions. Additionally, as a major endogenous antioxidant GSH, high levels of GSH in the tumor microenvironment protect tumor cells from oxidative stress, hence weakening the effect of PDT. Nevertheless, Cu(II)/Cu(I)-based MOFs and Mn-based MOFs are susceptible to redox reaction with GSH, decreasing intracellular GSH levels and increasing ROS levels simultaneously, which potentiate PDT effects.[102]

6.2.3 Constraining ACQ effects of photosensitizers. Most MOFs could be regarded as drug carriers, for instance, Zr-based MOFs and Zn-based MOFs, the steric hindrance effects of which inhibited the aggregation of loaded photosensitizers and potently restricted the ACQ phenomenon of photosensitizers. Meanwhile, the loaded substances were prone to diffusion owing to the special porous structure of MOFs, which improved the generation of ROS.[103] Additionally, some MOFs *per se* like Zr-based porphyrin-MOFs could be applied directly as a photosensitizer.

6.2.4 pH stimuli-responsive degradations. MOFs commonly reveal a pH-responsive property in the tumor microenvironment, ascribed to the weakly acidic nature of the tumor microenvironment and the central metal ions of the MOFs, which were favorable to expedite the decomposition of MOFs under acidic conditions and attain satisfactory drug release effects.[104] For instance, Chen *et al.*[105] constructed a pH-responsive zeolitic imidazolate framework-8-polyacrylic acid (ZIF-8-PAA) material

Table 2 Summary of the advantages and disadvantages of part MOF materials for PDT applications[83,85,87,90,107–109]

Categories of MOFs	Advantages	Disadvantages
Fe(II)/Fe(III)-based MOFs	Catalase-like function; alleviating hypoxic microenvironment; contrast agents for imaging; pH responsiveness; low toxicity	Poorly tumor specific targeting; narrow available spectral windows of common photosensitizers; metal toxicity
Cu(II)/Cu(I)-based MOFs	Directly acts as a photosensitizer; decreasing intracellular GSH levels; good biocompatibility; improving the permeability and retention (EPR) effect	Narrow available spectral windows of common photosensitizers; metal toxicity; having active surfaces that interact with biological agents
Zn-based MOFs	Decreasing intracellular GSH levels; pH responsiveness; satisfactory stability and biocompatibility;	Narrow available spectral windows of common photosensitizers; metal toxicity; having active surfaces that interact with biological agents
Zr-based MOFs	Alleviating hypoxic microenvironment; well preventing the self-polymerization and improving the dispersion in water; good biocompatibility	Narrow available spectral windows of common photosensitizers; metal toxicity; having active surfaces that interact with biological agents

encapsulating a broad-spectrum photosensitizer antibacterial agent ammonium methylbenzene blue (MB) for bacterial infection. The results have demonstrated that MB was released faster in MES buffer (pH 5.5) than in PBS buffer (pH 7.4), exhibiting an obvious pH-responsive property.

6.2.5 Good biocompatibility. In recent years, accumulating shreds of evidence have revealed that MOFs possess stable physicochemical properties *in vivo*.[106] They simultaneously exhibit low cytotoxicity, which is the critical factor of MOFs that can act as drug carriers in biomedical applications. For instance, Fu *et al.*[86] identified that ZIF-8@Ce6-HA has great biocompatibility, and the results indicated there are no abnormalities in hematological parameters. Similarly, Wang *et al.*[90] reported Zr-MOF@PPa/AF@PEG nanoparticles (NPs) had good biocompatibility and could achieve efficient antitumor effects based on the PDT-chemotherapy (CT) cascade process.

Briefly, MOFs are ideal candidates for addressing the dilemma of photodynamic therapy. We have summarized the advantages and disadvantages of part MOF materials for PDT applications in Table 2.

Taken together, MOFs offer the possibility of resolving the current two bottleneck issues of PDT. MOFs can co-load photosensitizers and chemotherapeutic drugs, which will release both counterparts to synergistically kill tumor cells after the degradation of MOFs in the tumor microenvironment.[110] The two-tailed logic can be fixed by monotonic MOFs, which may be regarded as a "synergy motor" for PDT (Fig. 7). We believe that this "synergy motor" has great prospects for enhancing the therapeutic efficacy of PDT, accelerating its wider clinical application.

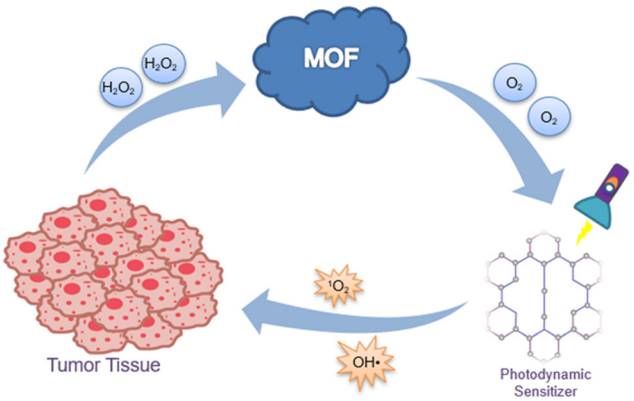

Fig. 7 "Synergy motor" MOFs for killing tumor cells.

7. Conclusions and foresight

Malignant tumors seriously endanger human health, and there is an increasing number of cancer patients. PDT is a promising treatment for malignant tumors, yet improvements should be urgently made to ensure its therapeutic efficacy. Traditional PDT only uses limited O_2 in the tumor microenvironment as the source of ROS, and the employed photosensitizers are susceptible to ACQ, which are the two major bottleneck issues for PDT application. MOFs are believed to hold promise in addressing the above-mentioned bottleneck issues of traditional PDT. They can transform the overexpressed endogenous H_2O_2 in tumor tissues into O_2 *via* Fenton/Fenton-like reactions. Moreover, the unique pores of the carrier could inhibit ACQ of photosensitizers through steric effects. Thus, such systems synergistically cope with the lack of O_2 and the low stability of the photosensitizer in the tumor microenvironment. MOFs are expected to achieve a breakthrough in PDT-based cancer clinical treatment.

It is also worth noticing that we need to screen the appropriate ions, which should not only ensure the activation of the Fenton reactions or Fenton-like reactions but also have a few side effects. The pore size of MOFs should also be considered to render them suitable for the loading of single or some photosensitizer molecules. Foremost, how to manufacture such systems on a large scale for promoting industrial translational research is another concern. We will make efforts to investigate these important issues in our future studies and pave the way for the commercialization of related products.

Author contributions

Meihong Zhang, paper writing, artworks preparation and literature survey; Yixian Zhou and Biyuan Wu, paper writing, conceptualization and literature survey; Chao Lu, Guilan Quan

and Zhengwei Huang, conceptualization, proof-reading and fund-seeking; Chuanbin Wu and Xin Pan, manuscript polishing and program management. The graphical abstract was drawn using Figdraw.

Conflicts of interest

Nothing to report.

Acknowledgements

This work was partially supported by the National Natural Science Foundation of China (82104070), the China Postdoctoral Science Foundation Special Funded Project (2022T150268) and the Guangzhou Science and Technology Plan Project (202201010589).

References

1 H. Sung, J. Ferlay, R. L. Siegel, M. Laversanne, I. Soerjomataram, A. Jemal and F. Bray, *Ca-Cancer J. Clin.*, 2021, **71**, 209–249.
2 O. Bakos, C. Lawson, S. Rouleau and L. H. Tai, *J. Immunother. Cancer*, 2018, **6**, 1–11.
3 Q. Ding, Z. Xu, L. Zhou, C. Rao, W. Li, M. Muddassir, H. Sakiyama, B. Li, Q. Qin and J. Liu, *J. Colloid Interface Sci.*, 2022, **621**, 180–194.
4 L. Barazzuol, R. P. Coppes and P. van Luijk, *Mol. Oncol.*, 2020, **14**, 1538–1554.
5 Y. Xu, Y. Tan, X. Ma, X. Jin, Y. Tian and M. J. M. Li, *Molecules*, 2021, **26**, 5990.
6 K. T. Kazantzis, K. Koutsonikoli, B. Mavroidi, M. Zachariadis, P. Alexiou, M. Pelecanou, K. Politopoulos, E. Alexandratou and M. Sagnou, *Photochem. Photobiol. Sci.*, 2020, **19**, 193–206.
7 D. K. Chatterjee, L. S. Fong and Y. Zhang, *Adv. Drug Delivery Rev.*, 2008, **60**, 1627–1637.
8 S. H. Voon, L. V. Kiew, H. B. Lee, S. H. Lim, M. I. Noordin, A. Kamkaew, K. Burgess and L. Y. J. S. Chung, *Small*, 2014, **10**, 4993–5013.
9 X. Li, S. Lee and J. Yoon, *Chem. Soc. Rev.*, 2018, **47**, 1174–1188.
10 H. Sies, V. V. Belousov, N. S. Chandel, M. J. Davies, D. P. Jones, G. E. Mann, M. P. Murphy, M. Yamamoto and C. Winterbourn, *Nat. Rev. Mol. Cell Biol.*, 2022, **23**, 499–515.
11 V. I. Lushchak, *Chem.-Biol. Interact.*, 2014, **224**, 164–175.
12 Z. J. Zhang, K. P. Wang, J. G. Mo, L. Xiong and Y. Wen, *World J. Stem Cells*, 2020, **12**, 562–584.
13 H. Yu, B. Chen, H. Huang, Z. He, J. Sun, G. Wang, X. Gu and B. Z. Tang, *Biosensors*, 2022, **12**, 348.
14 J. Li, Z. Zhuang, Z. Zhao and B. Z. Tang, *View*, 2021, **3**, 20200121.
15 L. Tan, X. Shen, Z. He and Y. Lu, *Front. Oncol.*, 2022, **12**, 863107.
16 M. Lismont, L. Dreesen and S. Wuttke, *Adv. Funct. Mater.*, 2017, **27**, 1606314.
17 W. Park, S. Cho, J. Han, H. Shin, K. Na, B. Lee and D.-H. Kim, *Biomater. Sci.*, 2018, **6**, 79–90.
18 T. P. Kubrak, P. Kołodziej, J. Sawicki, A. Mazur, K. Koziorowska and D. Aebisher, *Molecules*, 2022, **27**, 1192.
19 N. M. Carigga Gutierrez, N. Pujol-Sole, Q. Arifi, J. L. Coll, T. le Clainche and M. Broekgaarden, *Cancer Metastasis Rev.*, 2022, 1–36, DOI: 10.1007/s10555-022-10064-0.
20 W. Li, X. Guo, F. Kong, H. Zhang, L. Luo, Q. Li, C. Zhu, J. Yang, Y. Du and J. You, *J. Controlled Release*, 2017, **258**, 171–181.
21 J. Liu, H. Liang, M. Li, Z. Luo, J. Zhang, X. Guo and K. Cai, *Biomaterials*, 2018, **157**, 107–124.
22 I. S. Mfouo-Tynga, L. D. Dias, N. M. Inada and C. Kurachi, *Photodiagn. Photodyn. Ther.*, 2021, **34**, 102091.
23 Y. Qian, J. Wang, W. Bu, X. Zhu, P. Zhang, Y. Zhu, X. Fan and C. Wang, *Biomater. Sci.*, 2023, **11**, 704–718.
24 Y. Zhang, B.-T. Doan and G. Gasser, *Chem. Rev.*, 2023, **123**, 10135–10155.
25 K. Berg, P. Selbo, A. Weyergang, A. Dietze, L. Prasmickaite, A. Bonsted, B. Engesaeter, E. Angell-Petersen, T. Warloe and N. Frandsen, *J. Microsc.*, 2005, **218**, 133–147.
26 X. Zhao, J. Liu, J. Fan, H. Chao and X. Peng, *Chem. Soc. Rev.*, 2021, **50**, 4185–4219.
27 S. Kwiatkowski, B. Knap, D. Przystupski, J. Saczko, E. Kędzierska, K. Knap-Czop, J. Kotlińska, O. Michel, K. Kotowski and J. Kulbacka, *Biomed. Pharmacother.*, 2018, **106**, 1098–1107.
28 E. S. Nyman and P. H. Hynninen, *J. Photochem. Photobiol., B*, 2004, **73**, 1–28.
29 J. Xie, Y. Wang, W. Choi, P. Jangili, Y. Ge, Y. Xu, J. Kang, L. Liu, B. Zhang and Z. J. C. S. R. Xie, *Chem. Soc. Rev.*, 2021, **50**, 9152–9201.
30 K. Yan, Y. Zhang, C. Mu, Q. Xu, X. Jing, D. Wang, D. Dang, L. Meng and J. J. T. Ma, *Theranostics*, 2020, **10**, 7287.
31 J. J. A. C. I. E. Karges, *Angew. Chem., Int. Ed.*, 2022, **61**, e202112236.
32 J. Park, Y.-K. Lee, I.-K. Park and S. R. Hwang, *Biomedicines*, 2021, **9**, 85.
33 J. S. Souris, L. Leoni, H. J. Zhang, A. Pan, E. Tanios, H.-M. Tsai, I. V. Balyasnikova, M. Bissonnette and C.-T. Chen, *Nanomaterials*, 2023, **13**, 673.
34 W. Wang, E. Ma, P. Tao, X. Zhou, Y. Xing, L. Chen, Y. Zhang, J. Li, K. Xu and H. Wang, *J. Mater. Sci. Technol.*, 2023, **148**, 171–185.
35 X. Li, L. Chen, M. Huang, S. Zeng, J. Zheng, S. Peng, Y. Wang, H. Cheng and S. Li, *Asian J. Pharm. Sci.*, 2023, 100775.
36 Y. Duo, M. Suo, D. Zhu, Z. Li, Z. Zheng and B. Z. Tang, *ACS Appl. Mater. Interfaces*, 2022, **14**, 26394–26403.
37 Y. Li, D. Hu, M. Pan, Y. Qu, B. Chu, J. Liao, X. Zhou, Q. Liu, S. Cheng and Y. Chen, *Biomaterials*, 2022, **288**, 121700.
38 B. F. Jordan and P. Sonveaux, *Front. Pharmacol.*, 2012, **3**, 94.
39 Y. H. Cheng, H. Cheng, C. X. Jiang, X. F. Qiu, K. K. Wang, W. Huan, A. Yuan, J. H. Wu and Y. Q. Hu, *Nat. Commun.*, 2015, **6**, 1–8.
40 G. N. Masoud and W. Li, *Acta Pharm. Sin. B*, 2015, **5**, 378–389.
41 A. Marin-Hernandez, J. C. Gallardo-Perez, S. J. Ralph, S. Rodriguez-Enriquez and R. Moreno-Sanchez, *Mini-Rev. Med. Chem.*, 2009, **9**, 1084–1101.

42 F. Bolat, N. Haberal, N. Tunali, E. Aslan, N. Bal and I. Tuncer, *Pathol., Res. Pract.*, 2010, **206**, 19–23.
43 Q. Zhao, Y. Li, B. B. Tan, L. Q. Fan, P. G. Yang and Y. Tian, *PLoS One*, 2015, **10**, e0132746.
44 G. N. Masoud and W. Li, *Acta Pharm. Sin. B*, 2015, **5**, 378–389.
45 M. I. Koukourakis, A. Giatromanolaki, J. Skarlatos, L. Corti, S. Blandamura, M. Piazza, K. C. Gatter and A. L. Harris, *Cancer Res.*, 2001, **61**, 1830–1832.
46 S. Mitra, S. E. Cassar, D. J. Niles, J. A. Puskas, J. G. Frelinger and T. H. Foster, *Mol. Cancer Ther.*, 2006, **5**, 3268–3274.
47 Y. Z. Hu, K. Kirito, K. Yoshida, T. Mitsumori, K. Nakajima, Y. Nozaki, S. Hamanaka, T. Nagashima, M. Kunitama, K. Sakoe and N. Komatsu, *Mol. Cancer Ther.*, 2009, **8**, 2329–2338.
48 I. M. Pires, M. M. Olcina, S. Anbalagan, J. R. Pollard, P. M. Reaper, P. A. Charlton, W. G. McKenna and E. M. Hammond, *Br. J. Cancer*, 2012, **107**, 291–299.
49 Z. Zhang, M. Kang, H. Tan, N. Song, M. Li, P. Xiao, D. Yan, L. Zhang, D. Wang and B. Z. Tang, *Chem. Soc. Rev.*, 2022, **51**, 1983–2030.
50 W. Z. Yuan, P. Lu, S. M. Chen, J. W. Y. Lam, Z. M. Wang, Y. Liu, H. S. Kwok, Y. G. Ma and B. Z. Tang, *Adv. Mater.*, 2010, **22**, 2159–2163.
51 J. Qi, X. Hu, X. Dong, Y. Lu, H. Lu, W. Zhao and W. Wu, *Adv. Drug Delivery Rev.*, 2019, **143**, 206–225.
52 Y. Cheng, H. Cheng, C. Jiang, X. Qiu, K. Wang, W. Huan, A. Yuan, J. Wu and Y. Hu, *Nat. Commun.*, 2015, **6**, 1–8.
53 Z. Luo, M. Zheng, P. Zhao, Z. Chen, F. Siu, P. Gong, G. Gao, Z. Sheng, C. Zheng, Y. Ma and L. Cai, *Sci. Rep.*, 2016, **6**, 1–11.
54 D. Sheng, T. Liu, L. Deng, L. Zhang, X. Li, J. Xu, L. Hao, P. Li, H. Ran, H. Chen and Z. Wang, *Biomaterials*, 2018, **165**, 1–13.
55 C. M. C. Andrés, J. M. Pérez de la Lastra, C. A. Juan, F. J. Plou and E. Pérez-Lebeña, *Stresses*, 2022, **2**, 256–274.
56 C. Lennicke, J. Rahn, R. Lichtenfels, L. A. Wessjohann and B. Seliger, *Cell Commun. Signaling*, 2015, **13**, 1–19.
57 M. N. Wang, J. Z. Zhao, L. S. Zhang, F. Wei, Y. Lian, Y. F. Wu, Z. J. Gong, S. S. Zhang, J. D. Zhou, K. Cao, X. Y. Li, W. Xiong, G. Y. Li, Z. Y. Zeng and C. Guo, *J. Cancer*, 2017, **8**, 761–773.
58 H. J. Forman, A. Bernardo and K. J. A. Davies, *Arch. Biochem. Biophys.*, 2016, **603**, 48–53.
59 L. Jiao, W. Xu, H. Yan, Y. Wu, C. Liu, D. Du, Y. Lin and C. Zhu, *Anal. Chem.*, 2019, **91**, 11994–11999.
60 J. Tan, C. Sun, K. Xu, C. Wang and J. Guo, *Small*, 2015, **11**, 6338–6346.
61 C. Hu, Y. Yu, S. Chao, H. Zhu, Y. Pei, L. Chen and Z. Pei, *Molecules*, 2021, **26**, 3878.
62 Y. Feng, Y. Liu, X. Ma, L. Xu, D. Ding, L. Chen, Z. Wang, R. Qin, W. Sun and H. Chen, *J. Nanobiotechnol.*, 2022, **20**, 1–17.
63 Y. Gong, J. Leng, Z. Guo, P. Ji, X. Qi, Y. Meng, X. Z. Song and Z. Tan, *Chem. – Asian J.*, 2022, **17**, e202200392.
64 L. Y. Duan, Y. J. Wang, J. W. Liu, Y. M. Wang, N. Li and J. H. Jiang, *Chem. Commun.*, 2018, **54**, 8214–8217.
65 B. Kwon, E. Han, W. Yang, W. Cho, W. Yoo, J. Hwang, B. M. Kwon and D. Lee, *ACS Appl. Mater. Interfaces*, 2016, **8**, 5887–5897.
66 Y. S. Jung, W. T. Lim, J. Y. Park and Y. H. Kim, *Environ. Technol.*, 2009, **30**, 183–190.
67 D. Chen, Q. Xu, W. Wang, J. Shao, W. Huang and X. Dong, *Small*, 2021, **17**, e2006742.
68 H. Hu, L. Yu, X. Qian, Y. Chen, B. Chen and Y. Li, *Adv. Sci.*, 2021, **8**, 2000494.
69 Y. X. Ding, J. X. Wan, Z. H. Zhang, F. Wang, J. Guo and C. C. Wang, *ACS Appl. Mater. Interfaces*, 2018, **10**, 4439–4449.
70 K. Hao, L. Lin, P. Sun, Y. Hu, M. Atsushi, Z. Guo, H. Tian and X. Chen, *Small*, 2021, **17**, e2008125.
71 A. Rengaraj, P. Puthiaraj, Y. Haldorai, N. S. Heo, S.-K. Hwang, Y.-K. Han, S. Kwon, W.-S. Ahn and Y. S. Huh, *ACS Appl. Mater. Interfaces*, 2016, **8**, 8947–8955.
72 Z. Zhang, G. Quan, Q. Wu, C. Zhou, F. Li, X. Bai, G. Li, X. Pan and C. Wu, *Eur. J. Pharm. Biopharm.*, 2015, **92**, 28–31.
73 G. Quan, X. Pan, Z. Wang, Q. Wu, G. Li, L. Dian, B. Chen and C. Wu, *J. Nanobiotechnol.*, 2015, **13**, 1–12.
74 B. Y. Niu, Y. X. Zhou, T. Wen, G. L. Quan, V. Singh, X. Pan and C. B. Wu, *Colloids Surf., A*, 2018, **548**, 98–107.
75 K. Tu, J. Wu and W. Zhu, *RSC Adv.*, 2022, **12**, 29677–29687.
76 L. Feng, S. Gai, F. He, Y. Dai, C. Zhong, P. Yang and J. Lin, *Biomaterials*, 2017, **147**, 39–52.
77 Y. W. Hao, C. X. Zheng, H. Qiang, H. L. Chen, F. Wang, J. J. Zhang, H. L. Zhang, L. Wang, Z. Z. Zhang and Y. Zhang, *ChemNanoMat*, 2019, **5**, 1477–1487.
78 C. Yan, Y. Jin and C. Zhao, *Nanoscale Res. Lett.*, 2021, **16**, 1–8.
79 A. K. Kesharwani, R. Yadav and D. H. G. V. V. Sagar, *Int. J. Eng. Appl. Sci. Technol.*, 2022, **6**, 120–131.
80 Z. Mo, X. Pan, X. Pan, L. Ye, H. Hu, Q. Xu, X. Hu, Z. Xu, J. Xiong, G. Liao and S. Yang, *J. Mater. Chem. A*, 2022, **10**, 8760–8770.
81 M. Parsaei and K. Akhbari, *Inorg. Chem.*, 2022, **61**, 5912–5925.
82 S. Luo, Y. Zhao, K. Pan, Y. Zhou, G. Quan, X. Wen, X. Pan and C. Wu, *Biomater. Sci.*, 2021, **9**, 6772–6786.
83 Z. Liang, X. Li, X. Chen, J. Zhou, Y. Li, J. Peng, Z. Lin, G. Liu, X. Zeng and C. Li, *Front. Bioeng. Biotechnol.*, 2023, **11**, 1156079.
84 Y. Sun, X. Jiang, Y. Liu, D. Liu, C. Chen, C. Lu, S. Zhuang, A. Kumar and J. Liu, *J. Inorg. Biochem.*, 2021, **225**, 111599.
85 X. Cai, Z. Xie, B. Ding, S. Shao, S. Liang, M. Pang and J. Lin, *Adv. Sci.*, 2019, **6**, 1900848.
86 X. Fu, Z. Yang, T. Deng, J. Chen, Y. Wen, X. Fu, L. Zhou, Z. Zhu and C. Yu, *J. Mater. Chem. B*, 2020, **8**, 1481–1488.
87 M. Wang, F. Li, T. Lu, R. Wu, S. Yang and W. Chen, *Mater. Des.*, 2022, **224**, 111403.
88 Q. Zheng, X. Liu, Y. Zheng, K. W. Yeung, Z. Cui, Y. Liang, Z. Li, S. Zhu, X. Wang and S. Wu, *Chem. Soc. Rev.*, 2021, **50**, 5086–5125.
89 S. Karmakar, S. Barman, F. A. Rahimi and T. K. Maji, *Energy Environ. Sci.*, 2021, **14**, 2429–2440.

90 X. Wang, Z. Wang, W. Ma, X. Wu, W. Fang, C. Guo and Y. Jin, *J. Photochem. Photobiol., B*, 2021, **222**, 112274.
91 J. Chen, H. Niu, L. Guan, Z. Yang, Y. He, J. Zhao, C. Wu, Y. Wang, K. Lin and Y. Zhu, *Adv. Healthcare Mater.*, 2023, **12**, 2202474.
92 S. Y. Yin, G. Song, Y. Yang, Y. Zhao, P. Wang, L. M. Zhu, X. Yin and X. B. Zhang, *Adv. Funct. Mater.*, 2019, **29**, 1901417.
93 C. Li, J. Ye, X. Yang, S. Liu, Z. Zhang, J. Wang, K. Zhang, J. Xu, Y. Fu and P. Yang, *ACS Nano*, 2022, **16**, 18143–18156.
94 Y. Zhang, H. Fu, S. Chen, B. Liu, W. Sun and H. Gao, *Chem. Commun.*, 2020, **56**, 762–765.
95 X. Liu, Y. Jin, T. Liu, S. Yang, M. Zhou, W. Wang and H. Yu, *ACS Biomater. Sci. Eng.*, 2020, **6**, 4834–4845.
96 S. Wang, H. Wu, K. Sun, J. Hu, F. Chen, W. Liu, J. Chen, B. Sun and A. M. Hossain, *New J. Chem.*, 2021, **45**, 3271–3279.
97 Y. Ye, Y. Zhao, Y. Sun and J. Cao, *Int. J. Nanomed.*, 2022, 2367–2395.
98 M. R. Saeb, N. Rabiee, M. Mozafari and E. Mostafavi, *Materials*, 2021, **14**, 3652.
99 B. Maranescu and A. Visa, *Int. J. Mol. Sci.*, 2022, **23**, 4458.
100 X. Zhao, S. He, B. Li, B. Liu, Y. Shi, W. Cong, F. Gao, J. Li, F. Wang and K. Liu, *Nano Lett.*, 2023, **23**, 863–871.
101 F. Demir Duman, A. Monaco, R. Foulkes, C. R. Becer and R. S. Forgan, *ACS Appl. Nano Mater.*, 2022, **5**, 13862–13873.
102 X. Huang, X. Sun, W. Wang, Q. Shen, Q. Shen, X. Tang and J. Shao, *J. Mater. Chem. B*, 2021, **9**, 3756–3777.
103 Y. Ye, Y. Zhao, Y. Sun and J. Cao, *Int. J. Nanomed.*, 2022, 2367–2395.
104 X. Di, Z. Pei, Y. Pei and T. D. James, *Coord. Chem. Rev.*, 2023, **484**, 215098.
105 H. Chen, J. Yang, L. Sun, H. Zhang, Y. Guo, J. Qu, W. Jiang, W. Chen, J. Ji and Y. W. Yang, *Small*, 2019, **15**, 1903880.
106 C. Huang, M. Chen, L. Du, J. Xiang, D. Jiang and W. Liu, *Molecules*, 2022, **27**, 8386.
107 J. Hynek, M. K. Chahal, D. T. Payne, J. Labuta and J. P. Hill, *Coord. Chem. Rev.*, 2020, **425**, 213541.
108 Y. Sakamaki, J. Ozdemir, A. Diaz Perez, Z. Heidrick, O. Watson, M. Tsuji, C. Salmon, J. Batta-Mpouma, A. Azzun and V. Lomonte, *Adv. Ther.*, 2020, **3**, 2000029.
109 M. Ding, W. Liu and R. Gref, *Adv. Drug Delivery Rev.*, 2022, 114496.
110 Y. Chen, B. Wang, W. Chen, T. Wang, M. Li, Z. Shen, F. Wang, J. Jia, F. Li, X. Huang, J. Zhuang and N. Li, *Pharmaceutics*, 2022, **14**, 2047.